Polarimetric studies of L-arginine-doped potassium dihydrogen phosphate single crystals

Mykola Shopa, Yaroslav Shopa, Michael Shribak, Elena Kostenyukova, Igor Pritula and Olga Bezkrovnaya

IUCr Journals
CRYSTALLOGRAPHY JOURNALS ONLINE

Polarimetric studies of L-arginine-doped potassium dihydrogen phosphate single crystals

Mykola Shopa,[a]* Yaroslav Shopa,[b] Michael Shribak,[c] Elena Kostenyukova,[d] Igor Pritula[d] and Olga Bezkrovnaya[d]

[a]Department of Atomic, Molecular and Optical Physics, Gdańsk University of Technology, Narutowicza 11/12, Gdańsk 80-233, Poland, [b]Faculty of Mathematics and Natural Sciences, Cardinal Stefan Wyszyński University in Warsaw, Wóycickiego 1/3, Warsaw 01-938, Poland, [c]Marine Biological Laboratory, University of Chicago, 7 MBL Street, Woods Hole, MA 02543, USA, and [d]Institute for Single Crystals, NAS of Ukraine, Nauky Avenue 60, Kharkiv 61001, Ukraine. *Correspondence e-mail: mykola.shopa@pg.edu.pl

Conoscopic interference patterns, channelled spectra and polarimetric techniques have been used for the characterization of pure and doped (with L-arginine amino acid) potassium dihydrogen phosphate (KDP) single crystals. Experimental polarimetric data have been obtained for the frequently used wavelength of 633 nm and for two close wavelengths of 532 and 543 nm in a high-accuracy dual-wavelength polarimeter. The measurement of eigenwave ellipticity in the [100] and [010] directions and between 295 and 340 K shows small differences in the absolute values of the specific optical rotations of KDP crystals doped with L-arginine in the range of 0.7–3.8 wt%. It is found that the gyration tensor component g_{11}, specific optical rotation and eigenwave ellipticity show different dispersion in the visible spectral region.

1. Introduction

Potassium dihydrogen phosphate (KH_2PO_4, KDP) crystals have been known for decades and are still widely used as nonlinear and electro-optic materials (Authier, 2003; Dmitriev *et al.*, 2013; Rashkovich, 2019). The possibility of growing large single crystals of high optical quality stimulates the development of new devices and increases interest in fundamental research. In the past decade, KDP crystals doped with amino acids (in particular with L-arginine) have been studied in detail. The introduction of these organic molecules into the matrix of a KDP crystal improves the nonlinear optical parameters, increases the optical transparency and thermal stability, and decreases the electrical parameters (Krishnamurthy *et al.*, 2013; Parikh *et al.*, 2007; Muley *et al.*, 2009; Meena & Mahadevan, 2008). It has been observed that the efficiency of second-harmonic generation (SHG) in L-arginine (L-Arg)-doped crystals rises by a factor of about 2 in comparison with pure KDP (Parikh *et al.*, 2010; Kostenyukova *et al.*, 2016). Naturally, various experimental techniques have been used to characterize these materials, for example, X-ray diffraction, UV–visible–IR spectroscopy, and thermal and mechanical analyses (Kostenyukova *et al.*, 2019; Lavanya & Ravindran, 2019; Dolzhenkova *et al.*, 2017; Pritula *et al.*, 2016). It would be useful to supplement these techniques by the methods of optical anisotropy measurement applied to the above-mentioned doped crystals.

An apparatus for optical activity (OA) measurement along directions different from the optical axis direction, now known as the high-accuracy universal polarimeter (HAUP), was
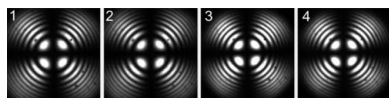
proposed a long time ago by Kobayashi *et al.* (1978) and Kobayashi & Vesu (1983), and the first objects of research on HAUP equipment were KDP crystals. Subsequently, these results became a standard for comparing the values of the OA of KDP crystals in other work (Takada *et al.*, 1989; Hernández-Rodríguez *et al.*, 2000; Shopa *et al.*, 2005). The ferroelectric properties of KDP crystals are also interesting, as witnessed by the important theoretical paper by Slater (1941), who explained the occurrence of ferroelectricity by the ordering of hydrogen bonds. Studies of the phenomenon of quadratic electrogyration at ambient temperature (Izdebski, 2019) and near the phase transition of the KDP crystal (Kobayashi *et al.*, 1988*b*) have also become vivid examples of the application of high-accuracy polarimetry in the physics of phase transitions.

We have previously reported high-accuracy polarimetry and electro-optic measurements with KDP doped with L-Arg (Shopa *et al.*, 2019). Our results did not reveal a noticeable dependence of OA on the concentration of L-Arg. In this paper, we have tried to study this problem more thoroughly using a dual-wavelength (532 and 543 nm) polarimeter, as well as a conventional polarimeter (633 nm). We have investigated the effect of L-Arg (0.7, 1.4 and 3.8 wt% of amino acid in the solution) on the OA, a phenomenon characterized by large anisotropy and sensitivity to structural changes of KDP-type single crystals (Shopa *et al.*, 2005).

2. Samples and experimental details

2.1. Conoscopic patterns and channelled spectra

Pure KDP and KDP:L-Arg crystals were grown from aqueous solutions by the temperature reduction method (Pritula *et al.*, 2016). X-ray diffraction studies of KDP and KDP:L-Arg crystals show variations in the lattice parameters at the level of only $\sim 10^{-4}$ Å, confirming the high quality of the crystals. No changes were observed in the external morphology of the L-Arg-doped KDP crystals, and only a slight blocking of the {100} faces compared with pure KDP was noted (Kostenyukova *et al.*, 2019).

The lowering of symmetry of doped crystals can also be detected in conoscopic interference patterns (Born & Wolf, 1999), so we applied the method of conoscopic studies to 0.5 mm thick (001)-cut samples. Using a two-coordinate optical stage and polarized light microscope, we were able to observe conoscopic patterns corresponding to $8 \times 8 = 64$ different positions of the sample with 10×10 mm cross

section. Fig. 1 demonstrates selected conoscopic patterns of KDP and KDP:L-Arg crystals recorded in monochromatic ($\lambda = 546$ nm) light. No noticeable distortions were observed for the doped crystals in comparison with the conoscopic pictures obtained for pure KDP. The ideal conoscopic pictures confirm the optical homogeneity of the samples and the high optical quality of the uniaxial optically inactive crystals along the [001] direction.

The channelled spectrum method (Ellis & Glatt, 1950; Hlubina & Ciprian, 2011) was used for comparison of the linear birefringence (LB) Δn of the studied crystals. (100)- and (010)-cut plates of equal thickness $d = 0.455$ mm were placed between crossed polarizers and illuminated by the light of a halogen lamp. The resulting fringes (Fig. 2) were recorded by a fibre-optic spectrometer to compare the LB dispersion across the visible spectrum.

The interference spectral minima satisfy the well known relation $(n_o - n_e)d = m\lambda$, where n_o and n_e are the ordinary and extraordinary refractive indices, respectively, and m is the order of the interference fringes which increases in the direction of shorter wavelengths λ. The number of fringes in these spectra for all three samples, including L-Arg-doped (3.8 wt%), is the same for the spectral region 450–800 nm.

The perceptible differences in channelled spectra between the *x*- and *y*-cut samples are comparable to those of the *y*-cut sample and 1.4 wt% L-Arg-doped KDP. The shift $\delta\lambda$ of channelled spectra observed for the (100) and (010) plates of pure KDP of uniform thickness is probably associated with small deviations in their orientation relative to the principal directions in the crystal. The changes in the birefringence $\Delta n = n_o - n_e$ values can be estimated using the relation $\delta(\Delta n) = m(\delta\lambda/d)$, and in the doped crystals were evaluated by us as a small increase of $\delta(\Delta n) \simeq 0.001$ near 450 nm and approximately 0.005 near 750 nm compared with the average birefringence for the [100] and [010] directions of pure KDP. Therefore, these data indicate a noticeable effect of doping of KDP crystals with L-arginine on the linear birefringence. At the same time, all polished samples were homogeneous and transparent, which allowed us to study their optical properties and in particular their OA.
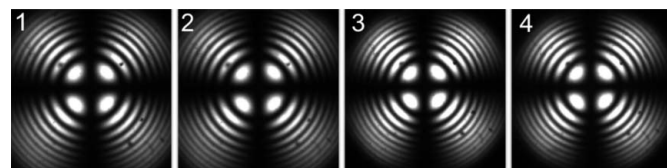

Figure 1
Selected conoscopic interference patterns viewed in monochromatic ($\lambda = 546$ nm) light along the optical axis of (1), (2) pure KDP and (3), (4) L-Arg-doped (3.8 wt%) KDP.
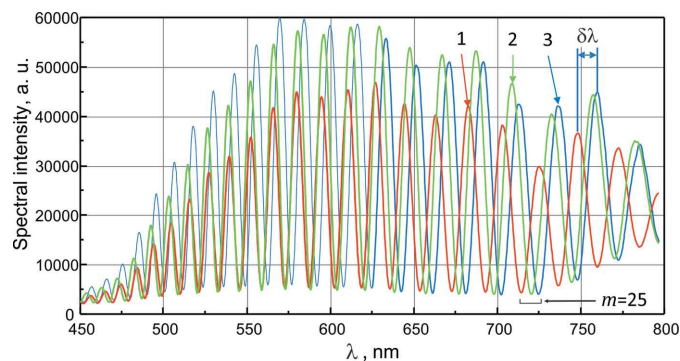

Figure 2
Three channelled spectra recorded using a fibre-optic spectrometer for samples of the same thickness $d = 0.455$ mm, (1) for (100) and (2) for (010) plates of pure KDP, and (3) for KDP:L-Arg (3.8 wt%). The order of the interference fringes near 720 nm is identified here as $m = 25$.

2.2. Conventional HAUP experiment

Since optical rotation for linearly polarized light propagating along the optical axis is forbidden by symmetry for point-group symmetry $\overline{4}2m$ (Nye, 1985), the OA can be measured in other directions where there is also LB. It is known that KDP crystals are levorotatory along the x axis and dextrorotatory along the y axis (Kaminsky et al., 2002). The main crystal optics parameter that relates to OA and can be measured experimentally is the eigenwave ellipticity k (Yariv & Yeh, 2002), the ratio of the minor axis to the major axis of the ellipse of eigenwave polarization. The ellipticity $k = \tan[G/(2\Delta n \overline{n})]$ depends on the ratio between the circular birefringence $G/\overline{n}$ and linear birefringence Δn. Here G is the scalar gyration parameter and $\overline{n}$ is the mean refractive index. For uniaxial crystals like KDP, perpendicular to the optical axis direction, circular birefringence is much smaller than linear birefringence ($G/\overline{n} \ll \Delta n$) so one can use the simple relation $G = 2k\Delta n \overline{n}$. In KDP crystals the k value does not exceed 4×10^{-4} (Shopa et al., 2005; Nichols et al., 2016) and its measurement is associated with certain difficulties.

In order to measure the influence of L-arginine doping on the OA of KDP single crystals, we used a fully automated laser polarimeter, which is very similar to the HAUP (Kobayashi & Vesu, 1983). In high-accuracy polarimetry, the sample is placed between nearly crossed polarizers in which the polarizer azimuth θ and analyser azimuth χ are small ($\theta, \chi \ll 1$) relative to the principal axis of the sample. In the equations below, it is assumed that with crossed polarizers and a zero input azimuth of the polarizer ($\theta = 0$), the analyser azimuth is also zero ($\chi = 0$). Under these conditions, the transmitted intensity $I(\theta, \chi)$ of the polarizer–sample–analyser (PSA) system can be written in the form of an elliptic paraboloid,

$$J(\theta, \chi) = A\theta^2 + 2B\theta\chi + C\chi^2 + 2D\theta + 2F\chi + H. \quad (1)$$

For the conditions of our experiment, $A = C = 1$, $B = -\cos\Gamma$, $D = (a + k)\sin\Gamma - \delta\chi\cos\Gamma$, $F = (p - k)\sin\Gamma + \delta\chi$ and $H = 0$, $\Gamma = (2\pi/\lambda)\Delta nd$ is the phase difference or retardation, λ is the wavelength of light, and d is the specimen thickness. One should also consider the imperfections of the polarizers, which are introduced as small ellipticities p and a of the light that passes through the polarizer and analyser, respectively. The angular error $\delta\chi$ in the determination of the crossed polarizers must also be taken into account (Kobayashi et al., 1988a; Kremers & Meekes, 1995; Folcia et al., 1999; Hernández-Rodríguez et al., 2000).

For the PSA system the analyser azimuth $\chi_{\min}^{PSA}$ that corresponds to the minimum light transmission, i.e. $(\partial J/\partial\chi)_\theta = 0$, can be expressed as (Shopa et al., 2017a)

$$\chi_{\min}^{PSA}(\theta, \Gamma) = (\theta + \delta\theta)\cos\Gamma + (k - p)\sin\Gamma - \delta\chi. \quad (2)$$

This makes it easy to measure the cosine of the phase differences Γ since, in a (θ, χ) coordinate system, the intensity minimum azimuths of the analyser are on a straight line with the tangent of the slope angle for each wavelength equal to $\cos\Gamma$. Note that the origin points of the measured azimuths

(θ', χ') differ from the true azimuths (θ, χ) by an unknown additive value $\delta\theta$.

Three characteristic polarizer azimuths are easily found experimentally for a paraboloid in the form given by (1). The expressions for these azimuths are as follows (Shopa et al., 2017b):

$$\theta_0' = (k - p)\cot\left(\frac{\Gamma}{2}\right) - \frac{\delta\chi}{1 - \cos\Gamma} + \delta\theta, \quad (3)$$

$$\theta_1' = (k - p)\cot\Gamma - \frac{k + a}{\sin\Gamma} + \delta\theta, \quad (4)$$

$$\theta_2' = -\frac{p + a}{2}\cot\left(\frac{\Gamma}{2}\right) - \frac{\delta\chi}{2} + \delta\theta. \quad (5)$$

They contain six unknown quantities (Γ, k, p, a, $\delta\chi$ and $\delta\theta$) that depend on the wavelength and cannot be determined under static experimental conditions. However, only the eigenwave ellipticity k and phase difference Γ are temperature dependent. It is also possible to change the crystal set in the polarization system after rotation of the sample by 90° around the optical axis of the polarimetric setup (Kobayashi et al., 1988a). The signs of k and Γ in expressions (2)–(5) should be reversed while p and a can be considered unchanged. This, however, does not solve the problem, since a new crystal set also changes the additive $\delta\theta$ and $\delta\chi$ values. To eliminate $\delta\theta$ it is sufficient to use the difference $\Delta\theta_{ij} = \theta_i' - \theta_j'$ (here $i = 0, 1, 2$) between the characteristic azimuths. It also appears that, even though the characteristic azimuths θ_i are measured independently, they are analytically related to each other, in particular

$$\Delta\theta_{01}\sin\Gamma = 2\Delta\theta_{02}\tan(\Gamma/2) = 2k - p + a - \delta\chi\cot(\Gamma/2), \quad (6)$$

$$\Delta\theta_{01}(1 - \cos\Gamma) = -2\Delta\theta_{12} = (2k - p + a)\tan(\Gamma/2) - \delta\chi. \quad (7)$$

Therefore, it is theoretically enough to measure only two of the azimuths θ_i' or one of the three differences $\Delta\theta_{ij}$. From an experimental point of view, the last two relations are important, since they make it possible to evaluate the quality of the data obtained on the polarimeter, in particular $\cos\Gamma$ according to formula (2) and the characteristic azimuth differences $\Delta\theta_{ij}$ according to relations (6) and (7).

The experimentally measured dependence of $\Delta_{01} = \Delta\theta_{01}\sin\Gamma$ on $\cot(\Gamma/2)$ for two sample sets is shown in Fig. 3. The data were obtained for the (100) plates of pure and doped KDP crystals at a wavelength $\lambda = 633$ nm. The change in the phase difference Γ was achieved by heating the samples from 300 to 350 K. The ellipticity k of the eigenwaves was considered constant since the very weak temperature dependence of the OA of KDP crystals at room temperature was confirmed earlier both experimentally (Takada et al., 1989; Shopa et al., 2005) and theoretically (Stasyuk et al., 1988). This simplifies the processing of the experimental results and makes it possible to determine systematic errors by linear approximation following relations (6) and (7).
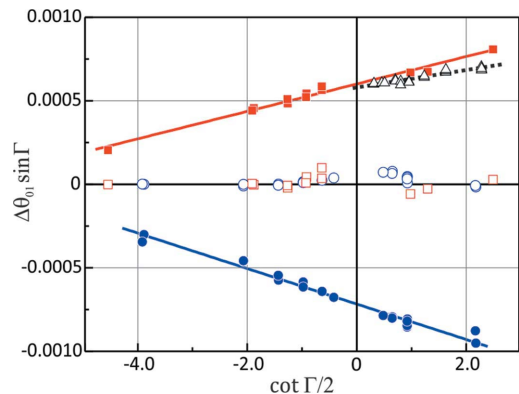
Figure 3
The dependencies of the characteristic values $\Delta\theta_{01}\sin\Gamma$ (solid symbols) and $\Delta\theta_{err}$ (open symbols) versus $\cot\Gamma/2$ for two KDP crystal sets in the PSA system ($\lambda = 633$ nm): $0°$ set (blue solid and open circles) and $90°$ set (red solid and open squares). Solid lines represent the best linear fits to the experimental data. One of the similar dependencies for a KDP:3.8 wt% L-Arg crystal is also shown (open triangles and dashed line).

As follows from Fig. 3, the average absolute value of the angular error $\delta\chi = (9.4 \pm 0.4) \times 10^{-5}$. Assuming that the eigenwave ellipticity k has reversed its sign after rotation of the sample by $90°$, from the intercept values of the two linear approximations we can determine the relatively minor effect of the parasitic ellipticities of the polarizers $p - a = (5.7 \pm 0.6) \times 10^{-5}$ and find the eigenwave ellipticity $k = (33.0 \pm 0.6) \times 10^{-5}$. Also, the error

$$\Delta_{err} = \Delta\theta_{01}\sin\Gamma - 2\Delta\theta_{02}\tan(\Gamma/2) \qquad (8)$$

in determining the characteristic values from relations (6) and (7) is insignificant, and this is shown in Fig. 3 for both sample sets. The corresponding measurement for the KDP:3.8 wt% L-Arg crystal gives the value $k = (34.0 \pm 0.8) \times 10^{-5}$. As follows from these data, within experimental error, the conventional high-accuracy polarimetric method for a wavelength $\lambda = 633$ nm does not allow one to detect the effect of doping on the OA of KDP crystals.

2.3. Dual-wavelength polarimetric studies

There are multiple extensions and improvements of the HAUP technique, such as the high-accuracy spectro-polarimeter (Moxon *et al.*, 1991), the generalized high-accuracy universal polarimeter (Asahi & Tanaka, 2012) and the fast-type high-accuracy universal polarimeter (Takanabe *et al.*, 2017). There are also other sensitive polarimeter approaches capable of solving similar problems based on other principles of the determination of polarization state changes of light, in particular the tilter polarimeter (Kaminsky & Glazer, 1996; Mucha *et al.*, 1997), the complete Muller matrix polarimeter (Arteaga *et al.*, 2009, 2012) and measuring OA in reflection (Arteaga, 2015).

An extended method for determining the eigenwave ellipticity k value and circular birefringence in a dual-wavelength polarimeter was described in detail in our previous work
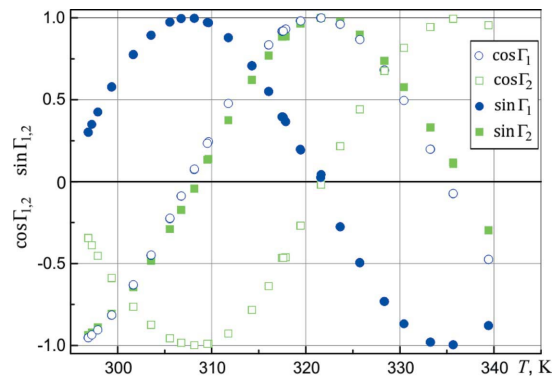

Figure 4
The temperature dependencies of the $\cos\Gamma_{1,2}$ (open symbols) and $\sin\Gamma_{1,2}$ (solid symbols) values for the 0.455 mm thick (100) plate of KDP doped with 3.8 wt% L-Arg for $\lambda_1 = 532$ nm (blue open and solid circles) and $\lambda_2 = 543$ nm (green open and solid squares).

(Shopa *et al.*, 2017a,b; Shopa & Ftomyn, 2018). In the current study we used the most common diode-pumped solid-state green laser ($\lambda_1 = 532$ nm) and a helium–neon laser ($\lambda_2 = 543$ nm) with relatively close wavelengths.

It is very important here to estimate the impact of the finite linewidth $\Delta\lambda$ of the laser on the measured $\cos\Gamma$ values during the experiment. Considering that, from the retardation definition of Γ, an increment $\Delta(\cos\Gamma)$ is given by

$$\Delta(\cos\Gamma) = \left(\frac{2\pi}{\lambda^2}\Delta nd\sin\Gamma\right)\Delta\lambda, \qquad (9)$$

and also assuming that the tolerable absolute value $\Delta(\cos\Gamma) < 0.002$, for KDP-type crystals we get that the $\cos\Gamma_1(\lambda_1)$ and $\cos\Gamma_2(\lambda_2)$ values should be measured accurately enough, provided that $\Delta\lambda < 0.005$ nm for $d = 0.5$ mm sample thickness. It is noteworthy that a helium–neon gas laser is preferred for use in the dual-wavelength polarimeter rather than the fairly common laser diode with a wide variety of wavelengths. Typically, the measured dependencies of $\cos\Gamma_{1,2}$ in Fig. 4 indicate the good wavelength stability of both lasers. For close wavelengths ($\lambda_2 - \lambda_1 = 11$ nm) there is a clear shift in the temperature dependencies of the $\cos\Gamma_{1,2}$ and $\sin\Gamma_{1,2}$ values.

For the processing of the experimental results, as seen from expressions (2)–(5), it is also necessary to obtain $\sin\Gamma_{1,2}$ correctly, which, unlike $\cos\Gamma_{1,2}$, are odd functions of the phase differences Γ. We have acquired the necessary data from the channelled spectra, from which the birefringence values, and therefore the phase differences Γ, decrease with increasing temperature of the samples. Based on this property of KDP crystals, the $\sin\Gamma_{1,2}$ dependencies become definite, and they are presented in Fig. 4. It is also possible to calculate the other trigonometric functions that are contained within the system of relations (2)–(5) and to derive the sign of the eigenwave ellipticity k. The last procedure is similar to that described by Lingard & Renshaw (1994).

An example of using several laser wavelengths for a broad spectrum in the HAUP technique was considered by Kobayashi *et al.* (1996). Assuming that k is independent of λ,

the authors of that work found the optimum values of the systematic errors and then calculated the wavelength dependence of k, which fortunately proved to be very close to zero.

We have applied only two lasers with close wavelength values λ_1 and λ_2, and this allows us to neglect the dispersion of the eigenwave ellipticity k value and also assume the systematic errors p, a and $\delta\chi$ to be constant. We have measured all the characteristic values alternately for both wavelengths at a fixed temperature of the crystal and with other experimental conditions uniform. As a result, a simpler solution of the systematic error elimination becomes possible. Since the additive $\delta\theta$ value in (3)–(5) is the same for both wavelengths, we can obtain three new differences $\Delta\theta_i = \theta_i(\lambda_1) - \theta_i(\lambda_2)$ between the characteristic azimuths θ_i ($i = 0, 1, 2$):

$$
\Delta\theta_0 = (k - p)\left[\cot\left(\frac{\Gamma_1}{2}\right) - \cot\left(\frac{\Gamma_2}{2}\right)\right] \\
- \delta\chi\left[(1 - \cos\Gamma_1)^{-1} - (1 - \cos\Gamma_2)^{-1}\right], \quad (10)
$$

$$
\Delta\theta_1 = (k - p)(\cot\Gamma_1 - \cot\Gamma_2) - (k + a)\left(\frac{1}{\sin\Gamma_1} - \frac{1}{\sin\Gamma_2}\right), \\
(11)
$$

$$
\Delta\theta_2 = -\frac{p + a}{2}\left[\cot\left(\frac{\Gamma_1}{2}\right) - \cot\left(\frac{\Gamma_2}{2}\right)\right]. \quad (12)
$$

Considering also the possibility of two crystal sets (0 and 90° optical axis orientation relative to the maximum transmission plane of the polarizer) in the PSA system, the number of equations which can be used to calculate the eigenwave ellipticity k and eliminate the systematic errors p, a and $\delta\chi$ is doubled. Note here that, in accepting the invariability of the systematic errors, one should take care to ensure minimal

changes in the laser beam passing through the elements of the polarimeter. At the same time, uncontrolled rotation of the crystal during heating in a thermostat is not critical here.

To simplify the analysis of the experimental results based on the relationships given by equations (10)–(12), from now on we will use the following notation:

$$
A_0 = \cot\left(\frac{\Gamma_1}{2}\right) - \cot\left(\frac{\Gamma_2}{2}\right), \\
B_0 = (1 - \cos\Gamma_1)^{-1} - (1 - \cos\Gamma_2)^{-1}, \\
A_1 = \cot\Gamma_1 - \cot\Gamma_2, \\
B_1 = \frac{1}{\sin\Gamma_1} - \frac{1}{\sin\Gamma_2}. \quad (13)
$$

Considering that $\Delta\theta_0/B_0 = (k - p)A_0/B_0 - \delta\chi$, it is more convenient to consider the linear dependencies of the characteristic values $\Delta\theta_0/B_0$ on the A_0/B_0 ratio. Examples of three such dependencies for pure and doped KDP crystals are shown in Fig. 5. Following the symmetry properties of KDP crystals, the slope of the straight line for the (010)-cut sample has the opposite sign to the (100)-cut sample, while A_0/B_0 does not change its sign after rotation of the crystal.

The linear fits to the collected experimental data, like those presented in Fig. 5, allowed us to obtain for each sample two $k - p$ values (corresponding to two crystal sets and opposite signs of k), which are averaged over the thermal (295–340 K) and spectral (532–543 nm) intervals. From the intercept values in Fig. 5, we also found that the absolute magnitude of the systematic error $\delta\chi < 0.02 \times 10^{-3}$ and is within the standard error of the linear fit.

Similarly to the previous consideration, we used relation (11) and obtained a linear dependence between characteristic values of the $\Delta\theta_{1\lambda}/A_1$ and B_1/A_1 ratios for each temperature of the sample, i.e. $\Delta\theta_{1\lambda}/A_1 = k - p - (k + a)B_1/A_1$. The two linear dependencies for the (100) and (010) plates of pure KDP crystal are shown in Fig. 6. As we can see, the slopes of these
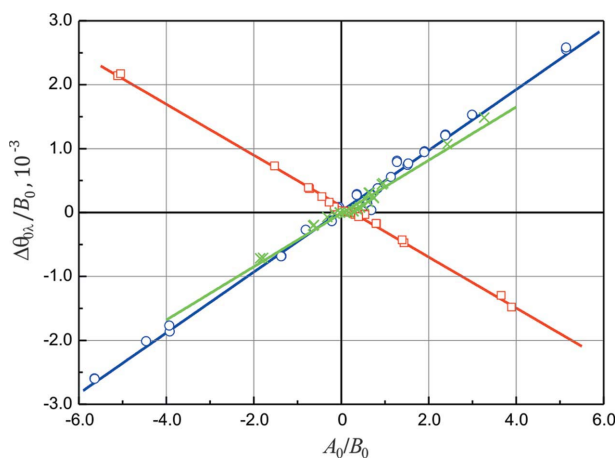

Figure 5
Three plots of the $\Delta\theta_{0\,\lambda}/B_0$ values versus A_0/B_0 ratio for the (010) plate of pure KDP (red open squares) and for the (100) plates of 1.4 wt% (green crosses) and 3.8 wt% (blue open circles) L-Arg-doped KDP crystals. Solid lines represent the best fits to the experimental data and give from their slopes $k - p = -(0.42 \pm 0.02) \times 10^{-3}$ for the (100) plate of 1.4 wt% L-Arg-doped KDP, $k - p = -(0.47 \pm 0.03) \times 10^{-3}$ for the (100) plate of 3.8 wt% L-Arg-doped KDP and $k - p = (0.40 \pm 0.01) \times 10^{-3}$ for the (010) plate of pure KDP.
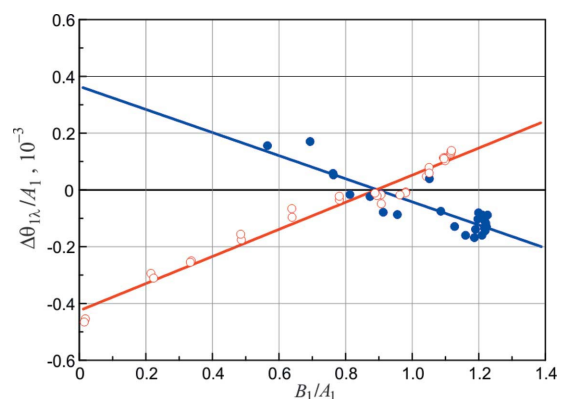

Figure 6
Two plots of the $\Delta\theta_{1\lambda}/A_1$ characteristic values versus B_1/A_1 ratio for the (100) (red open circles) and (010) (blue solid circles) plates of the pure KDP crystal. The slopes of the fitted lines are equal to $-k - a = (0.48 \pm 0.02) \times 10^{-3}$ for the (100) plate and $-k - a = -(0.41 \pm 0.05) \times 10^{-3}$ for the (010) plate. The intercepts of the fitted lines give $k - p = -(0.43 \pm 0.05) \times 10^{-3}$ and $(0.36 \pm 0.02) \times 10^{-3}$, respectively.
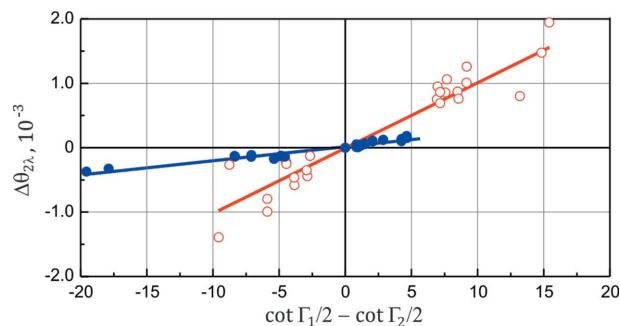
Figure 7
The dependency of one of the characteristic angle differences $\Delta\theta_2$ on $\cot(\Gamma_1/2) - \cot(\Gamma_2/2)$ for pure KDP (red open circles) and 3.8 wt% L-Arg-doped (blue solid circles) samples. The lines of the best fits give from their slopes $-(p + a)/2 = (0.10 \pm 0.08) \times 10^{-3}$ for pure KDP and $-(p + a)/2 = (0.022 \pm 0.010) \times 10^{-3}$ for 3.8 wt% L-Arg-doped KDP.
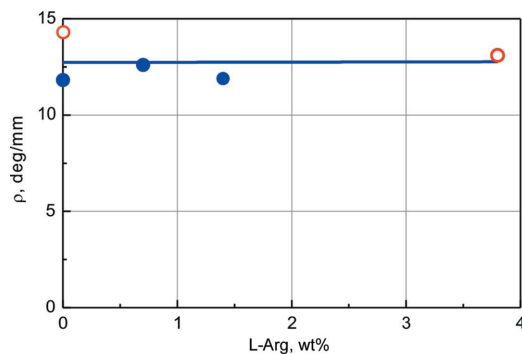

Figure 8
Absolute rotatory power value for pure and L-Arg-doped KDP crystals for the (100) (blue solid circles) and (010) (red open circles) crystal plates and an average wavelength of 536 nm.

lines, as well as the intersection points, carry information about the required parameters k, p and a.

Finally, using the third expression (12) for characteristic differences, we found that $\Delta\theta_2 = -A_0(p + a)/2$. This dependence contains only the sum of the parasitic ellipticities of the polarizer and analyser. The intercept values in Fig. 7 are very close to the origin and are an indirect verification of the correctness of the used expressions. Thus, for two crystal sets in the PSA system and three characteristic polarizer azimuth differences, we have obtained enough data to find the systematic errors p, a and $\delta\chi$ and calculate the eigenwave ellipticity k values. We should note that in the dual-wavelength polarimetric experiment it is not necessary to determine the angular error $\delta\chi$ since it is absent from expressions (11) and (12) and can only serve as a quality indicator of the mechatronic parts of the polarimeter.

As we have seen, determination of the systematic error plays an important role in HAUP experiments, which was confirmed by other authors (Kremers & Meekes, 1995; Folcia et al., 1999; Hernández-Rodríguez et al., 2000; Herreros-Cedrés et al., 2002). It was repeatedly noted that such a parameter as the parasitic ellipticity of the polarizers (p and a) is essentially an indicator of the sample quality rather than the quality of the polarization prism itself. Therefore, it is very difficult to measure OA in crystals grown by the Czochralski method and it is not surprising that measurements with different samples give dissimilar values of systematic errors and the data for those same crystals are different, such as for langasite ($La_3Ga_5SiO_{14}$) [see, for comparison, Kaminskii et al. (1983), Shopa & Kravchuk (1996) and Shopa et al. (2017a)].

3. Optical activity and dispersion

The scheme described in the previous section for obtaining experimental results on the dual-wavelength polarimeter was applied to each of the mentioned crystals. Some data are duplicated, because according to equations (10) and (11), the eigenwave ellipticity k can be calculated from the slope of one straight line (see Fig. 5) and also from the intercept and slope

of another (see Fig. 6). This allows us to improve the accuracy by using the mean values in the calculations and avoid experimental errors.

Fig. 8 presents the results of the dual-wavelength measurements that we made on five samples of pure and doped KDP crystals. Each point in the figure was obtained for the two crystal sets in the polarization system and corresponds to the average wavelength of 536 nm for the dual-wavelength polarimeter. The grown crystals have well developed {100} and {010} growth sectors, but the correct identification of the crystallographic axes is impossible without measurement of physical effects similar to OA, which, according to the symmetry, should be manifested in different ways in the [100] and [010] directions. We used (100) and (010) crystal plates and confirmed the opposite signs of the OA in the x and y directions, assuming that, according to the conventions used by Kaminsky et al. (2002), the [010] direction is dextrorotatory and the eigenwave ellipticity $k > 0$. Within the accuracy of our experiments, the effect of doping on the OA of KDP crystals is insignificant. This can be explained by the weak influence of L-arginine on the OA.

Having obtained the eigenwave ellipticity for the two wavelengths (536 and 633 nm), we considered the dispersion of parameters related to the OA based on the coupled oscillator model originating with Born (1935). According to the theory of Chandrasekhar (1961) and Vysín (1966), the rotatory dispersion formulas along and normal to the optical axis are of the same form. Note that only the eigenwave ellipticity k value is directly measured experimentally, while the magnitude of the circular birefringence ($G/\overline{n}$), the gyration tensor component $g_{11} = 2k\Delta n\overline{n}$ (or scalar gyration parameter G) and the optical rotatory power $\rho = (\pi/\lambda n_e)g_{11}$ are obtained from formulas containing the mean refractive index $\overline{n}$, the linear birefringence Δn and the light wavelength λ. Naturally, it would be incorrect to apply the same forms of the dispersion equation for these different crystal-optical quantities. We see such arguments in the work of Arteaga et al. (2009) for the example of a quartz crystal, suggesting another expression to parameterize the g_{11} component. In our case, a classical one-term Drude formula of the type

$$g_{11} = \frac{A}{\lambda^2 - \lambda_0^2} \qquad (14)$$

is best suited to the experimental data (Fig. 9, curve 1). Here $A = 1.478 \times 10^{-5}\ \mu m^2$ is the parameter to be determined for a wavelength of 633 nm and the characteristic absorption wavelength $\lambda_0 = 0.0991\ \mu m$ that can be obtained for the refractive index dispersion (Zernike, 1964), based on the single-term Sellmeier equation [see, for example, Koralewski & Surma (1980)]. Next, using the formula

$$\rho = \frac{B\lambda^2}{\left(\lambda^2 - \lambda_0^2\right)^2}, \qquad (15)$$

we found that it does not fit for the rotatory power ρ (Fig. 9, curve 2). We note here that, in the visible spectral region, the differences in the dependencies that are built on relations (14) and (15) are relatively minor. At the same time, the formula proposed by Arteaga et al. (2009),

$$k = \frac{B\lambda^3}{\left(\lambda^2 - \lambda_0^2\right)^2}, \qquad (16)$$

is the most suitable to describe the dispersion of the eigenwave ellipticity k (Fig. 9, curve 3).

One should also remember that the classical models of the dispersion of OA were developed mainly for quartz crystals and were refined on the basis of accurate measurements of the absorption and rotatory power along the optical axis over a wide spectral region. By contrast, we have obtained experimental data for only two wavelengths in the visible spectral region. The value $g_{11} = 4.00 \times 10^{-5}$ for the wavelength of 633 nm is in good agreement with the measured data that are given by Hernández-Rodríguez et al. (2000) and Kaminsky et al. (2002). Unfortunately, we do not have the capability for polarimetric measurements at lower wavelengths, in particular in the UV region. The anisotropy of the absorption in

Figure 9
Experimental data for the KDP crystal of the gyration tensor component g_{11} (green open circles), optical rotatory power ρ (red crosses) and eigenwave ellipticity k (blue open squares) at wavelengths of 536 and 633 nm. The dispersions of the same quantities as calculated using equations (14), (15) and (16) are represented by solid lines 1, 2 and 3, respectively.

L-arginine-doped KDP crystals (Kostenyukova et al., 2019) may indicate the presence of linear dichroism, which is exhibited in any optically active molecule (Rodger, 2013). The differences in the dispersion of OA should be noticeable in this region, but polarimetric studies under such conditions are significantly more challenging. Linear and circular dichroism can be measured relatively easily if there is no linear bi-refringence, i.e. along the optical axis of the crystal. However, in KDP-type crystals along the z axis, this is forbidden by the symmetry conditions. The determination of OA in reflection close to the bandgap, proposed by Arteaga (2015), may be more suitable.

In the KDP group of crystals there are ample opportunities for varying chemical composition and deuteration (replacement of hydrogen by deuterium) without altering the symmetry, although the measurement of OA in the birefringent directions of these crystals is more complicated. The ionic, crystalline and mixed contributions to the gyration tensors from the various configurations of H_nPO_4 ionic groups have been considered theoretically for KDP crystals (Stasyuk et al., 1988). The configurations of H_nPO_4 groups are determined by the number and positions of the protons in the hydrogen bonds. As follows from this consideration, there is a summation of various contributions, mainly from H_2PO_4 ionic groups, which, according to Slater (1941), have the lowest energy. The significant role of the PO_4 atomic group is confirmed by a comparison of the absolute values of OA for some KDP-family crystals (Shopa et al., 2005). These studies have shown that the isomorphous replacement of K with Rb or NH_4 has a lesser impact on the OA than the replacement, for example, of PO_4 with AsO_4. It was discovered that OA in pure KDP-type crystals is associated with the chiral structure along the [100] and [010] axes, which is formed by the PO_4 groups (Koralewski & Surma, 1980; Kaminsky et al., 2002; Claborn et al., 2008).

At the same time, the nonlinear coefficients vary slightly with isomorphic replacement in the KDP group of crystals (Eimerl, 1987) and a semi-classical model of the SHG in KDP is based on anharmonic oscillation of electrons in the PO_4 atomic group. The growth of the SHG efficiency in L-Arg-doped KDP may be influenced by the increase in electron density, because the amino acid contains an amino group with a strong electron-acceptor property.

Spectroscopic data for the IR region indicate the presence of absorption of hydrogen bonding between the phosphate unit of KDP and the amino group of L-arginine (Govani et al., 2009), and disturbance of the N—H, C—H and C—N bonds of the amino acid. We can assume that, maybe, there are not too many random spatial orientations of the molecules in the crystal network and only a few discrete placements that correspond to the creation of chemical bonds. Thus, there is a change in the environment of the asymmetric (chiral) carbon atom, which is attached to four different types of atoms or atom groups in L-arginine. Unfortunately, we cannot determine the nature of such changes and their effect on the chirality of the L-arginine molecules. We note that, in the crystalline state, the monoclinic crystals of L-arginine
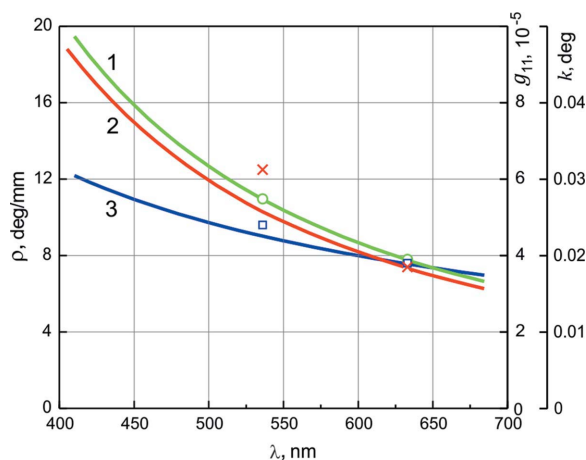
phosphate have nonlinear properties, they are optically active (Monaco *et al.*, 1987; Eimerl *et al.*, 1989) and they show a strong anisotropy of OA (Herreros-Cedrés *et al.*, 2003, 2005). Most likely, the small mass fraction of ʟ-arginine limits the possibility of detecting any change in the OA in doped KDP crystals within the framework of our experimental technique.

4. Conclusions

We have presented new characterization data of KDP crystals with organic additives introduced during the growth process that provide improvement of the nonlinear optical properties. The polarimetric technique applied in this work showed no correlation between optical nonlinearity and gyration properties in ʟ-arginine-doped KDP crystals. We have observed high optical homogeneity of the doped crystals using conoscopic interference patterns along the optical axis. A small biaxiality that can usually be seen as a lightening at the centre of the conoscopic pattern was not detected in any of the samples. The channelled spectra indicated only slight changes in the linear birefringence in the ʟ-arginine-doped crystals compared with pure KDP.

Although measurement of the optical activity of KDP crystals is associated with certain experimental difficulties, we have tried to detect changes due to the presence of dopants using two different high-accuracy polarimetric methods: a conventional high-accuracy polarimeter and a dual-wavelength polarimeter, which is a HAUP modification and not critically sensitive to systematic errors. Rotation of the sample by 90° and averaging data for two close wavelengths were applied to eliminate systematic errors in the HAUP technique. Despite the low level of systematic errors, the high quality of the crystals and measuring in two different crystallographic directions, according to these two methods the gyrotropic coefficients for pure and ʟ-arginine-doped KDP are approximately the same. Using these experimental data, the dispersion of the parameters related to the optical activity was calculated from the classic one-term formulas.

References

Arteaga, O. (2015). *Opt. Lett.* **40**, 4277–4280.
Arteaga, O., Canillas, A. & Jellison, G. E. Jr (2009). *Appl. Opt.* **48**, 5307–5317.
Arteaga, O., Freudenthal, J. & Kahr, B. (2012). *J. Appl. Cryst.* **45**, 279–291.
Asahi, T. & Tanaka, M. (2012). *Kobunshi*, **61**, 777–778.
Authier, A. (2003). Editor. *International Tables for Crystallography*, Vol. D, *Physical Properties of Crystals*. Dordrecht: Kluwer Academic Publishers.
Born, M. (1935). *Proc. R. Soc. London Ser. A*, **150**, 84–105.
Born, M. & Wolf, E. W. (1999). *Principles of Optics: Electromagnetic Theory of Propagation, Interference and Diffraction of Light.* Cambridge University Press.
Chandrasekhar, S. (1961). *Proc. R. Soc. London Ser. A*, **259**, 531–553.

Claborn, K., Isborn, C., Kaminsky, W. & Kahr, B. (2008). *Angew. Chem. Int. Ed.* **47**, 5706–5717.
Dmitriev, V. G., Gurzadyan, G. G. & Nikogosyan, D. N. (2013). *Handbook of Nonlinear Optical Crystals.* Heidelberg: Springer.
Dolzhenkova, E. F., Kostenyukova, E. I., Bezkrovnaya, O. N. & Pritula, I. M. (2017). *J. Cryst. Growth*, **478**, 111–116.
Eimerl, D. (1987). *Ferroelectrics*, **72**, 95–139.
Eimerl, D., Velsko, S., Davis, L., Wang, F., Loiacono, G. & Kennedy, G. (1989). *IEEE J. Quantum Electron.* **25**, 179–193.
Ellis, J. W. & Glatt, L. (1950). *J. Opt. Soc. Am.* **40**, 141–142.
Folcia, C. L., Ortega, J. & Etxebarria, J. (1999). *J. Phys. D Appl. Phys.* **32**, 2266–2277.
Govani, J., Durrer, W., Manciu, M., Botez, C. & Manciu, F. (2009). *J. Mater. Res.* **24**, 2316–2320.
Hernández-Rodríguez, C., Gómez-Garrido, P. & Veintemillas, S. (2000). *J. Appl. Cryst.* **33**, 938–946.
Herreros-Cedrés, J., Hernández-Rodríguez, C., González-Díaz, B. & Guerrero-Lemus, R. (2003). *Appl. Phys. B*, **77**, 607–612.
Herreros-Cedrés, J., Hernández-Rodríguez, C. & Guerrero-Lemus, R. (2002). *J. Appl. Cryst.* **35**, 228–232.
Herreros-Cedrés, J., Hernández-Rodríguez, C. & Guerrero-Lemus, R. (2005). *Mater. Sci. Forum*, **480–481**, 43–52.
Hlubina, P. & Ciprian, D. (2011). *Opt. Commun.* **284**, 2683–2686.
Izdebski, M. (2019). *J. Appl. Cryst.* **52**, 158–167.
Kaminskii, A. A., Mill, B. V., Khodzhabagyan, G. G., Konstantinova, A. F., Okorochkov, A. I. & Silvestrova, I. M. (1983). *Phys. Status Solidi A*, **80**, 387–398.
Kaminsky, W. & Glazer, A. M. (1996). *Ferroelectrics*, **183**, 133–141.
Kaminsky, W., Haussühl, E., Bastin, L. D., Anand Subramony, J. & Kahr, B. (2002). *J. Cryst. Growth*, **234**, 523–528.
Kobayashi, J., Asahi, T., Sakurai, M., Takahashi, M., Okubo, K. & Enomoto, Y. (1996). *Phys. Rev. B*, **53**, 11784–11795.
Kobayashi, J., Asahi, T., Takahashi, S. & Glazer, A. M. (1988*a*). *J. Appl. Cryst.* **21**, 479–484.
Kobayashi, J., Takada, M., Hosogaya, N. & Someya, T. (1988*b*). *Ferroelectr. Lett. Sect.* **8**, 145–152.
Kobayashi, J., Takahashi, T., Hosokawa, T. & Uesu, Y. (1978). *J. Appl. Phys.* **49**, 809–815.
Kobayashi, J. & Uesu, Y. (1983). *J. Appl. Cryst.* **16**, 204–211.
Koralewski, M. & Surma, M. (1980). *Phys. Status Solidi A*, **58**, K59–K62.
Kostenyukova, E. I., Bezkrovnaya, O. N., Kolybaeva, M. I., Dolzhenkova, E. F., Kovalenko, N. O., Kanaev, A. & Pritula, I. M. (2016). *Funct. Mater.* **23**, 27–31.
Kostenyukova, E., Pritula, I., Bezkrovnaya, O., Kovalenko, N., Doroshenko, A., Khimchenko, S. & Fedorov, A. (2019). *Semicond. Phys. Quantum Electron. Optoelectron.* **22**, 60–66.
Kremers, M. & Meekes, H. (1995). *J. Phys. D Appl. Phys.* **28**, 1195–1211.
Krishnamurthy, R., Rajasekaran, R. & Samuel, B. S. (2013). *Spectrochim. Acta A Mol. Biomol. Spectrosc.* **104**, 310–314.
Lavanya, N. & Ravindran, B. (2019). *Res. Rev.* **4**, 845–851.
Lingard, R. J. & Renshaw, A. R. (1994). *J. Appl. Cryst.* **27**, 647–649.
Meena, M. & Mahadevan, C. K. (2008). *Cryst. Res. Technol.* **43**, 166–172.
Monaco, S. B., Davis, L. E., Velsko, S. P., Wang, F. T., Eimerl, D. & Zalkin, A. (1987). *J. Cryst. Growth*, **85**, 252–255.
Moxon, J. R. L., Renshaw, A. R. & Tebbutt, I. J. (1991). *J. Phys. D Appl. Phys.* **24**, 1187–1192.
Mucha, D., Stadnicka, K., Kaminsky, W. & Glazer, A. M. (1997). *J. Phys. Condens. Matter*, **9**, 10829–10842.
Muley, G. G., Rode, M. N. & Pawar, B. H. (2009). *Acta Phys. Pol. A*, **116**, 1033–1038.
Nichols, S., Martin, A., Choi, J. & Kahr, B. (2016). *Chirality*, **28**, 460–465.
Nye, J. (1985). *Physical Properties of Crystals.* Oxford University Press.
Parikh, K. D., Dave, D. J., Parekh, B. B. & Joshi, M. J. (2007). *Bull. Mater. Sci.* **30**, 105–112.

Parikh, K. D., Dave, D. J., Parekh, B. B. & Joshi, M. J. (2010). *Cryst. Res. Technol.* **45**, 603–610.

Pritula, I. M., Kostenyukova, E. I., Bezkrovnaya, O. N., Kolybaeva, M. I., Sofronov, D. S., Dolzhenkova, E. F., Kanaev, A. & Tsurikov, V. (2016). *Opt. Mater.* **57**, 217–224.

Rashkovich, L. N. (2019). *KDP-Family Single Crystals.* Boca Raton: CRC Press.

Rodger, A. (2013). *Polarized Light, Linear Dichroism, and Circular Dichroism.* In *Encyclopedia of Biophysics*, edited by G. C. K. Roberts. Heidelberg: Springer.

Shopa, M. & Ftomyn, N. (2018). *Opt. Eng.* **57**, 034101.

Shopa, M., Ftomyn, N. & Shopa, Y. (2017a). *J. Opt. Soc. Am. A*, **34**, 943–948.

Shopa, M., Shopa, Y., Kostenyukova, E., Pritula, I. & Bezkrovnaya, O. (2019). *Opt. Laser Technol.* **119**, 105655.

Shopa, Y. & Kravchuk, M. (1996). *Phys. Status Solidi. A*, **158**, 275–280.

Shopa, Y., Lutsiv-Shumskiy, L. & Serkiz, R. (2005). *Ferroelectrics*, **317**, 79–82.

Shopa, Y., Shopa, M. & Ftomyn, N. (2017b). *Opto-Electron. Rev.* **25**, 6–9.

Slater, J. C. (1941). *J. Chem. Phys.* **9**, 16–33.

Stasyuk, I. V., Kotsur, S. S. & Stetsiv, R. Y. (1988). *Ferroelectr. Lett. Sect.* **8**, 71–74.

Takada, M., Hosogaya, N., Someya, T. & Kobayashi, J. (1989). *Ferroelectrics*, **96**, 295–300.

Takanabe, A., Koshima, H. & Asahi, T. (2017). *AIP Adv.* **7**, 025209.

Vysín, V. (1966). *Proc. Phys. Soc.* **87**, 55–60.

Yariv, A. & Yeh, P. (2002). *Optical Waves in Crystals: Propagation and Control of Laser Radiation.* Chichester: Wiley.

Zernike, F. (1964). *J. Opt. Soc. Am.* **54**, 1215–1220.

Mykola Shopa *et al.* • L-Arginine-doped KDP single crystals **1265**